NANO LETTERS

pubs.acs.org/NanoLett Letter

Size-Dependent Lattice Symmetry Breaking Determines the Exciton Fine Structure of Perovskite Nanocrystals

Daniel Weinberg,* Yoonjae Park,* David T. Limmer,* and Eran Rabani*

Cite This: *Nano Lett.* 2023, 23, 4997−5003 Read Online

ACCESS | Metrics & More | Article Recommendations | Supporting Information

ABSTRACT: The order of bright and dark excitonic states in lead-halide perovskite nanocrystals is debated. It has been proposed that the Rashba effect, driven by lattice-induced symmetry breaking, causes a bright excitonic ground state. Direct measurements of excitonic spectra, however, show the signatures of a dark ground state, bringing the role of the Rashba effect into question. We use an atomistic theory to model the exciton fine structure of perovskite nanocrystals, accounting for realistic lattice distortions. We calculate optical gaps and excitonic features that compare favorably with experimental works. The exciton fine structure splittings show a nonmonotonic size dependence due to a structural transition between cubic and orthorhombic phases. Additionally, the excitonic ground state is found to be dark with spin triplet character, exhibiting a small Rashba coupling. We additionally explore the effects of nanocrystal shape on the fine structure, clarifying observations on polydisperse nanocrystals.

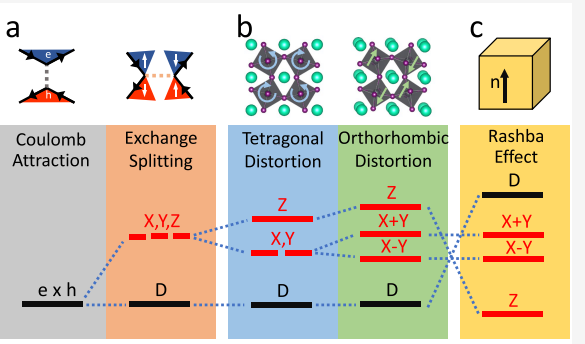

KEYWORDS: *Perovskites, Nanocrystals, Excitons, Exciton fine structure, Rashba effect, Lattice symmetry*

Lead-halide perovskite nanocrystals (NCs) have attracted significant attention due to their remarkable optical and electronic properties that could lend themselves to diverse applications.[1−3] Perhaps most interestingly, these materials show remarkably fast radiative lifetimes, which shorten at low temperatures in contrast to other nanomaterials.[4−10] This anomalous temperature dependence of the radiative lifetimes has led to speculation that these materials could exhibit a reversal of the typical exciton fine structure (FS) measured in all other nanomaterials to date.[5,11,12] Specifically, Becker et al.[5] proposed that the lowest excitonic state is a bright state, i.e., that it has an optically allowed transition to the material ground state. If that is the case, at low temperatures, the carriers will preferentially be in the bright, rapidly emissive state rather than depend on thermal fluctuations to reach an emissive state. Understanding the excitonic FS in these materials is important to assess their suitability as quantum light sources, which depends in part on the uniquely fast radiative lifetimes.[13−16] The argument for a bright excitonic ground state was supported by a detailed analysis of the physics of excitons in perovskite NCs from an effective mass model. We will briefly revisit this before describing our atomistic approach to this problem, which can provide a definitive ordering of bright and dark states in lead-halide perovskite NCs.

In the typical picture, electrons and holes are bound into excitons by their strong Coloumbic attraction forming a hydrogenic series of states that may be modified by confinement effects of the NC.[17] For systems with negligible spin−orbit coupling, the electron and hole spins are decoupled from the spatial degrees of freedom and simple addition of angular momentum describes the resulting triplet and singlet spin functions. The electron−hole exchange interaction slightly reduces the strength of exciton binding for excitons with spin-singlet character, introducing a spin dependence into the exciton FS. Notably, for materials like perovskites with significant spin−orbit coupling, the spatial and spin degrees of freedom are not separable. Further, it is known that the excited state properties of the perovskites are sensitive to the lattice structure, as the charge-lattice coupling in these materials is significant.[18−21]

In the specific case of the perovskite NCs studied here, the conduction band is composed mainly of of Pb-6p orbitals which are strongly split by spin−orbit coupling. The conduction band edge is composed of the $J = 1/2$ total angular momentum subspace formed from the addition of the spin and the orbital angular momentum. The valence band has s-type symmetry and thus is not split by spin−orbit coupling.[22] In the exciton, this causes the exchange interaction to split three bright states with mixed spin-triplet and spin-singlet

Received: March 6, 2023
Revised: May 15, 2023
Published: May 25, 2023

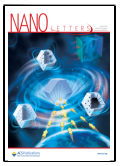

https://doi.org/10.1021/acs.nanolett.3c00861
Nano Lett. 2023, 23, 4997−5003

character above a dark ground state with pure spin-triplet character. These bright states each have dipoles polarized normal to one of the nanocrystal facets, corresponding to the ⟨100⟩ family of directions in the cubic lattice and which we take as the Cartesian principle axes. For such a cubic crystalline structure these three bright states are perfectly degenerate and are often referred to as "bright triplets" due to their total angular momentum triplet character, however this should not be confused with their spin character.

Any deviation from this cubic structure will result in splitting among these bright states. Perovskite materials are known to progress through a series of symmetry lowering phase transitions as temperature is reduced,[23,24] and Figure 1b

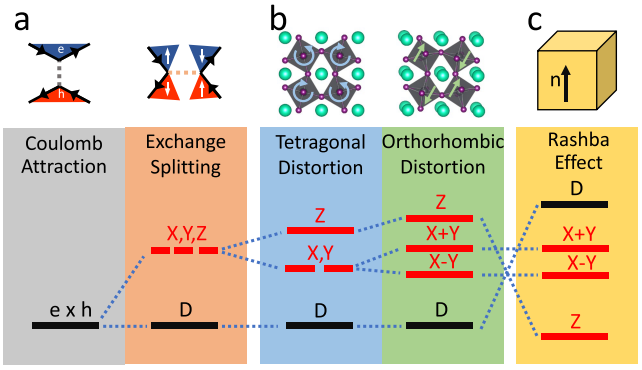

Figure 1. (a) Effects of electron−hole interaction, (b) lattice distortion, and (c) the previously proposed[5] role of the Rashba effect on the exciton FS. Adapted from ref 12. Copyright 2019 American Chemical Society.

illustrates the effect of these distortions on the exciton FS. A tetragonal distortion caused by rotation of the lead-halide octahedra around the z-axis splits the z-oriented state higher in energy, but the symmetry in the x−y plane maintains the degeneracy of those two states. At lower temperatures, tilting of the octahedra breaks that symmetry and further splits the bright states in the x−y plane into two states polarized at 45° angle to the principle axes.[25] These symmetry lowering splittings are observed experimentally as a splitting of the excitonic emission into two or three distinct lines,[5,7,26] but on their own they do not lead to a reversal of the bright-dark level ordering.

The theorized bright ground state may be arrived at through the influence of the Rashba effect.[27] This additional term in the **k·p** Hamiltonian comes from the coexistence of strong spin−orbit coupling and inversion symmetry breaking. The additional "effective exchange"[5] term only enters the Hamiltonian through two parameters− a magnitude and direction along which inversion symmetry is broken. This, by nature, is blind to the atomistic detail of the symmetry breaking at the nanoscale, and leaves unknown the exact nature of a NC structure that would give rise to such a level ordering.

In fact, several recent measurements[7,26,28] have detected a signature of a dark ground state several meVs below the bright states. Under the influence of a external magnetic field, the Zeeman effect couples dark states to energetically close bright states, resulting in an emergent emission line. Under these conditions the dark ground state can be directly observed. The FS splittings are instead explained in terms of the interplay of crystal structure and NC shape anisotropy.[26]

Various theoretical attempts have been made to provide additional understanding of atomistic detail of this effect, as well as provide tools to understand how to disentangle the Rashba effect, the crystal field splitting, and NC shape anisotropy to determine the level ordering and splitting in these NCs. Within an effective mass model, the Rashba splitting as indicated by the energy difference between Z and X/Y excitons is predicted to increase to the bulk limit with increasing NC size.[12] On the other hand, the effect of shape anisotropy should be lesser for larger NCs.[29] This does, however, lead to a troubling question: If the Rashba effect is more pronounced for larger NCs, but absent in the bulk, where would the transition to more bulk-like behavior occur? The resolution of this must come from an atomistic theory that can also describe how the structure of small NCs may be distorted and how that of large NCs converges to the bulk limit. These questions involving the Rashba effect have also been considered in the context of 2D layered perovskites, where theoretical studies using both phenomenological[30] and Bethe−Salpeter equation (BSE)-based[31] models of the electron−hole exchange interaction show that specific polar lattice distortions may be sufficient to cause a bright excitonic ground state. On the other hand, a recent theoretical investigation focusing on methylammonium lead iodide considered the effect of methylammonium relaxation within a fixed tetragonal lead iodide framework and found only weak a Rashba effect insufficient to cause level inversion.[32]

To fully understand the intertwined roles of the Rashba effect and lattice symmetry, we must consider the full structure of perovskite NCs in atomistic detail, especially including the lead halide framework that contributes most strongly to the valence and conduction band states. To do this, we use a previously developed atomistic force field[33] to find the lowest energy configuration for a series of $CsPbI_3$ perovskite NCs shown in Figure 2a. The bulk properties of this model have been extensively validated.[34,35] As the measurements of the exctionic FS occur at cryogenic temperatures, these single minimized structures accurately represent the atomic configuration of the NCs in these experiments, and the effects of

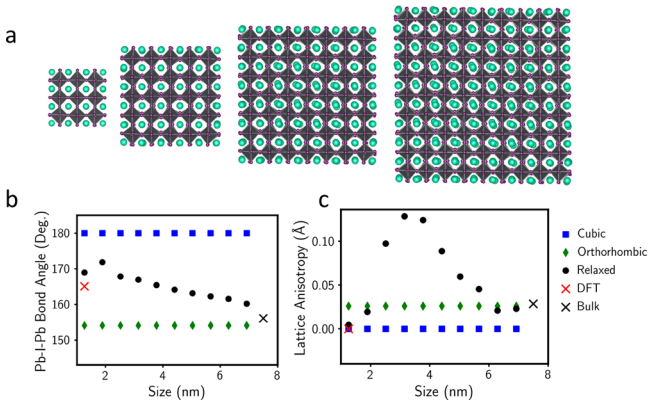

Figure 2. (a) Renderings of 1.9, 3.1, 4.4, and 5.7 nm $CsPbI_3$ NC cubes after structural relaxation. Cs atoms are shown in teal, I atoms are shown in purple, and Pb atoms are shown as gray coordination octahedra. (b) Average Pb−I−Pb bond angle and (c) the extent of lattice anisotropy induced by the relaxation for cubic (blue squares), orthorhombic (green diamonds), and relaxed (black circles) structures. Red and black × symbols represent the results from DFT calculation and bulk simulation, respectively.

https://doi.org/10.1021/acs.nanolett.3c00861
Nano Lett. 2023, 23, 4997−5003

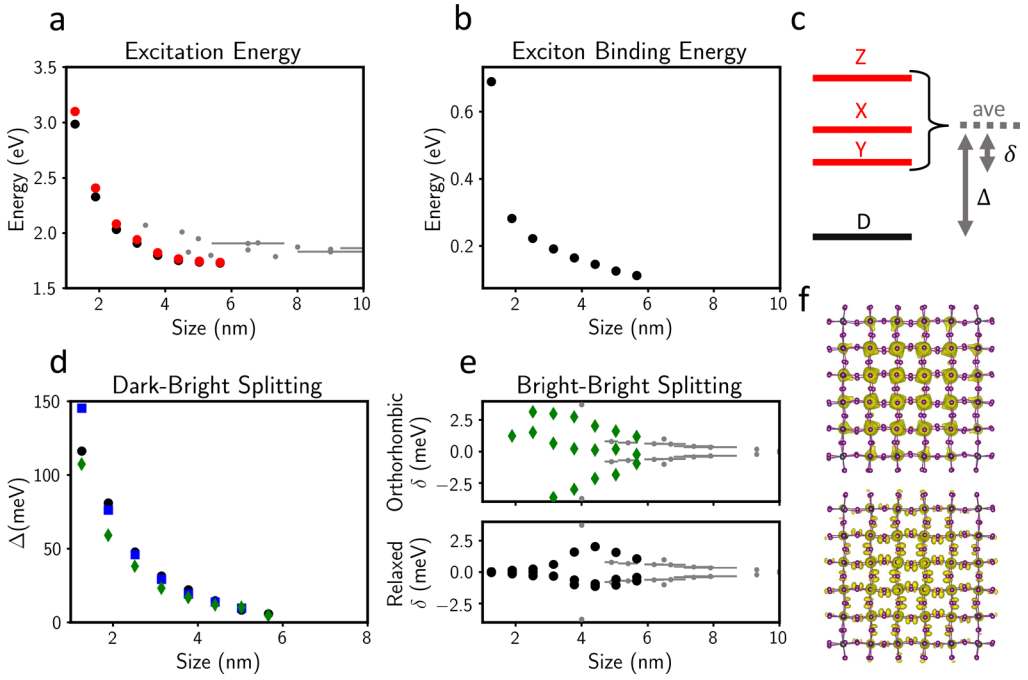

Figure 3. (a) Lowest bright (red) and dark (black) excitonic states for relaxed NCs as a function of size along with experimental data.[36,45−49] (b) Exciton binding energies ignoring dielectric confinement effects[50,51] for relaxed NCs as a function of size. (c) Level diagram describing the splittings calculated. (d) Calculated splitting between the bright and dark excitonic states. (e) Splitting among the bright excitonic states for orthorhombic (top, green diamonds) and relaxed (bottom, black circles) NCs with experimental splittings.[10,25,52,53] (f) Electron density plots for the HOMO (bottom) and LUMO (top) states.

lattice dynamics may be ignored. The relaxed structures can be compared to the bulk cubic and orthorhombic structures on the basis of the average Pb−I−Pb bond angles. These are shown in Figure 2b and reveal that these relaxed structures lie somewhere between the cubic and orthorhombic structures. The cubic structures have no octahedral rotation and therefore all bond angles are 180 deg. For the orthorhombic structures the significant octahedral rotation leads to an average bond angle of 154 degrees. The smallest relaxed structures take more cubic forms, but the larger ones approach the orthorhombic configuration which is the stable bulk structure.

To quantify the extent to which the NC relaxation breaks crystal symmetries we define a lattice anisotropy parameter. It is defined by taking the average of the Pb−Pb distances along each of the principal axes, and then finding the difference between the direction with the lowest average and the direction with the highest average. We plot this parameter against NC size in Figure 2c. For the cubic structures, this is always zero, and for the orthorhombic structures the elongated *z*-axis gives a small constant anisotropy. The small relaxed structures are highly symmetric so this anisotropy is near zero, but as the size increases beyond 2 nm in size, octahedral rotations begin to emerge. These are not uniform throughout the NC, however, and remain suppressed at the surface leading to significant lattice anisotropy. Significant deviation from the cubic crystal structure is not unexpected, as although cubic phase QDs have been stabilized at room temperature and somewhat below,[36] the cryogenic temperatures at which the FS measurements take place should favor the orthorhombic structure. The size-dependent effect has been observed experimentally,[37] and is driven by a competition between surface energy and bulk phase stability which had been previously explored using a continuum model.[38] The predicted phase crossover around 2.7 nm aligns well with the region of highest lattice anisotropy. Additionally, for both average bond angle and lattice anisotropy parameter, the results from the smallest and largest nanocrystals agree well with the results from DFT calculation and bulk CsPbI3 simulation, respectively, which lends confidence to our ability to produce an atomistic description of complex structural behavior at the nanoscale. This size dependent effect has not previously been considered in the context of the exciton FS, and will play a crucial role in understanding the size dependence of the FS splittings.

Obtaining the exciton FS from these relaxed NC configurations requires an electronic structure method that is responsive to the atomistic detail of the material. While these materials are too large for *ab initio* theories such as DFT combined with many-body perturbation techniques, semiempirical methods are able to access the size ranges necessary. We employ the semiempirical pseudopotential method,[39−42] which assigns each atom in the NC an effective potential derived from bulk band structures. These pseudopotentials include both local and nonlocal components that capture the effect of spin−orbit coupling. As our relaxed NCs lie somewhere in between the cubic and orthorhombic crystal phases, pseudopotentials have been fit to describe the band structures of both phases individually. The pseudopotentials used in the NC calculations are linearly interpolated between these, based on the local NC structure. This way, the electronic structure is sensitive to local deformations or distortions in the lattice. The optical absorption spectrum is computed using the BSE within the static screening approximation, which describes the bound excitonic states in the basis of free electron−hole pairs.[43,44] This approach allows for equal treatment of the direct and exchange terms in a nonperturbative manner, and

https://doi.org/10.1021/acs.nanolett.3c00861
Nano Lett. 2023, 23, 4997−5003

fully takes into account the effects of spin−orbit coupling. This treatment is essential to determining the full excitonic spectrum of these NCs and the FS splitting. Additional details on the electronic calculations can be found in the Supporting Information.

We can evaluate the success of this method by comparing the computed optical gaps to a wide range of experimental results. In Figure 3a, we show the lowest excitonic states (dark and bright) of the relaxed NCs across a range of sizes. The excitation energies for the cubic and orthorhombic structures are plotted in Figure S6, and show a strong agreement with experimental PL measurements.[36,45,46,48,49] The relaxed structures show a stronger confinement effect, with the smallest NCs having higher excitation energies than the other structures due to the effects of relaxation on the angles between lead halide octahedra. The smallest relaxed structures differ significantly from either the cubic or orthorhombic geometries, and this forces the electron and hole quasiparticle states further apart in energy, opening the optical gap. For the larger NCs, the effect is the opposite as the optical gaps fall somewhat below that of the other structures and experiments. This can be understood through the simple bonding and antibonding picture of the bulk lead halide perovskites band structure. In the bulk, the upper valence band consists of antibonding states between Pb-6s and I-5p orbitals, and the lower conduction band consists of antibonding states between Pb-6p and I-5p orbitals, dominated by the Pb-6p orbitals.[22,54,55]

In the NCs, the hole and electron quasi-orbitals (shown in Figure 3f) maintain much of their bulk character. For the smallest relaxed NCs, the Pb−I bond lengths are at a maximum, decreasing their antibonding interaction and lowering the valence band energy. The Pb−Pb distance is also exceptionally long lessening their interaction and pushing the conduction band higher in energy. This distortion changes character once the NCs pass the critical threshold of 3−4 nm in length where octahedral tilting brings the Pb atoms closer together, and the decreased Pb−I−Pb bond angle somewhat lessens the antibonding interaction. This brings the valence band quasiparticle energies into line with those of the orthorhombic structures, but the decreased Pb−Pb distances still drive the conduction band to fall below that of the fully orthorhombic structures.

While the relaxation has some impact on the overall excitation energies, Figure 3d shows that it has little to no impact on the splitting between dark and bright states. For the cubic, orthorhombic, and relaxed structures studied, the ground state exciton remains dark up to 6 nm NCs, and the trend with increasing size shows that a positive dark-bright splitting is expected for all sizes of NCs. This is consistent with the recent calculations by Biffi et al.[32] which considered $MAPbI_3$ NC with atomistic electronic theory while only allowing relaxation of the MA cations. We find that expanding the relaxation to the lead halide octahedral backbone does not result in a level inversion and does not support a strong Rashba effect in these materials. If either relaxation, or the enforcement of an orthorhombic crystal structure caused a significant Rashba effect, then the dark-bright splitting would be qualitatively different from that of the cubic structures which always have inversion symmetry and thus no Rashba effect.

A deeper understanding of the exciton FS can come from investigating the spin statistics of the lowest excitonic states. While the total spin $\hat{S}_{tot}^{\ 2} = (\hat{\mathbf{S}}_e + \hat{\mathbf{S}}_h)^2$ need not be a good quantum number, the expectation value of the total spin will still be indicative of the degree of spin-singlet versus spin-triplet character. As shown in Figure S5, the total spin expectation value for the dark states is very close to 2, the value for a triplet state. The bright states have lower total spin, close to the value of $^4/_3$ predicted by effective mass theory,[12,29] indicative of a significant spin-singlet character. The implications of this can be understood through the expectation values of the exchange interaction for each of the states. Only the bright states, with their partial spin-singlet character, feel the effects of exchange. This spin structure is present in all the structures we consider, ensuring a dark excitonic ground state regardless of structural relaxation.

The crystal structure does, however, have a significant impact on the splitting among the bright states as seen in Figure 3e. The cubic structures are not shown as the bright levels are always degenerate. Considering the orthorhombic structures, the bright−bright splitting decreases with increasing NC size, contrary to the predictions of a model where the Rashba effect is sufficiently strong to cause a bright-dark inversion.[12] What is observed is consistent with a simple crystal-field splitting that would approach the bulk at large NC sizes.[56,57] The relaxed crystal structures are where we would expect to see signatures of the Rashba effect emerge if it was present, as the ions are allowed to relax and could strongly break inversion symmetry. These signatures are not present, and the complex behavior that we do see in the bright−bright splittings is due to the NC size dependent structural transition discussed earlier. The smallest NCs have more symmetric structures and thus smaller bright−bright splittings. For the larger NCs the structures become nearly orthorhombic and thus the splittings resemble those of the orthorhombic NCs. Both of these splittings match well to experiments,[7,10,25,52,53] although the lack of data for extremely small NCs make the predictions of the relaxed structures difficult to verify. Additional measurements of the exciton FS in extremely small perovskite NCs could help resolve questions of the structure of these smallest clusters.

The polarization dependent emission spectra can also be calculated from our atomistic theory. These spectra are shown in Figure S7 for NCs of various crystal structures all with 3.8 nm edge lengths. In agreement with the effective mass models, we observe only one peak for the cubic structure, lying around 20 meV above a dark ground state. For the orthorhombic structure, the splittings due to lattice distortion are clearly recovered and the polarization of the lower two excitonic states is aligned with the orthorhombic crystal axes rather than the faces of the NC, also in agreement with the effective mass models.[25] The spectra for the relaxed structures show similarities to the orthorhombic structure, but the lower two excitonic states are close enough in energy that they may not be resolvable into separate peaks. The results for the relaxed structures add the additional structural complexity not considered in an effective mass model. Taken as a whole, the results of our model conclusively show that the inversion symmetry breaking in perovskite NCs is not sufficient to produce a bright ground state.

While it is easy to simulate a perfectly cubic NC, experiments tend to produce a distribution of NCs that differ from the perfect cubic geometry. This NC shape anisotropy is also known to impact the excitonic FS and may be implicated

https://doi.org/10.1021/acs.nanolett.3c00861
Nano Lett. 2023, 23, 4997−5003

in the diversity of FS splittings observed experimentally.[26] In Figure 4, we consider the effect of shape anisotropy on NCs of

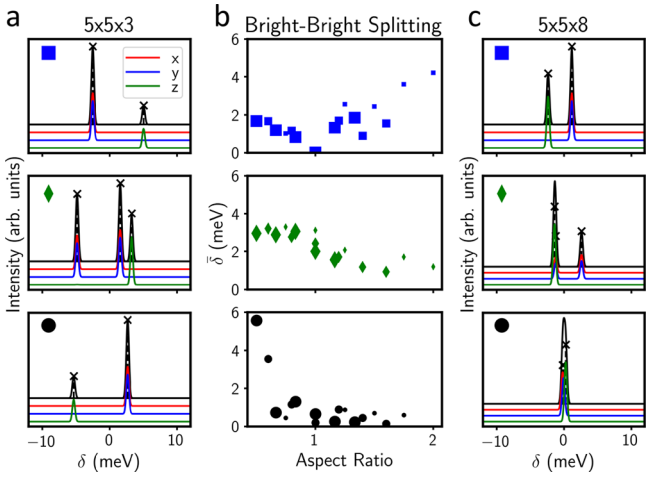

Figure 4. (b) Standard deviation of the bright excitonic states for the cubic (top), orthorhombic (middle), and relaxed (bottom) crystal structures. The sizes of the symbols represent the sizes of the NCs along the x and y directions. The largest symbols correspond to $N = 6$, and the smallest to $N = 4$. (a) Polarization-dependent spectra for NCs consisting $5 \times 5 \times 3$ lead-halide octahedra (aspect ratio of 0.6) and (c) $5 \times 5 \times 8$ octahedra (aspect ratio of 1.6) similarly arranged by crystal structure.

cubic, orthorhombic and relaxed crystal structures. We generated a series of NCs consisting of $N \times N \times Z$ lead-halide octahedra where $N = 4, 5, 6$ and $Z = 3, ..., 8$. We define the aspect ratio as Z/N, and in Figure 4b we plot the standard deviation of the bright states for each of these NCs. In Figure 4a and c, we show the polarization dependent spectra of the bright states for an aspect ratio less than 1 and greater than 1 respectively. For the NCs with cubic crystal structures the bright−bright splitting is zero for cube-shaped crystals, and either adding or removing layers from such a NCs causes a finite splitting. As the axis of shape anisotropy was chosen as the z-axis, the x- and y-polarized excitons remain degenerate, as seen in the plotted spectra. For an aspect ratio less than 1, the z-polarized exciton is split higher in energy. For an aspect ratio greater than 1, the z-polarized exciton is lower in energy than the x- or y-polarized ones. This behavior agrees well with what has been derived from various effective mass models.[7,25,26]

The NCs with an orthorhombic crystal structure show a significant degree of bright−bright splitting at all aspect ratios, consistent with effective mass theories.[7,25,26] Additionally, the extent to which the z-polarized exciton is split lower at large aspect ratio appears suppressed, as it can be seen to be essentially degenerate with the lower x/y-polarized exciton in the middle panel of Figure 4c. The relaxed structures show a unique behavior with significant bright−bright splittings at aspect ratios less than 1, which are due almost entirely to the z-polarized exciton splitting to lower energy. This behavior is the opposite of that observed in the orthorhombic and cubic phases, and may result from surface relaxation effects that become more dominant for plate-like geometries. At larger aspect ratios, the relaxed structures show small splitting that depends only weakly on aspect ratio. This may be due to the size-dependent effects discussed above. As single NC measurements remain extremely challenging, especially those correlated to NC shape data, understanding the exact impacts of NC shape anisotropy is still an experimental challenge.

In conclusion, we calculate the exciton FS for lead-halide perovskite NCs using a fully atomistic theory to obtain relaxed NC crystal structures and the electronic states of these relaxed NCs. The structural relaxation reveals in atomistic detail previously predicted structural transitions, and the electronic theory reproduces experimental optical gaps with excellent agreement. This atomistic theory would be able to discern the causes and nature of a Rashba effect caused by collective inversion symmetry breaking if it was present in these systems. None of the signatures of a significant Rashba effect are found in this study. For all NCs studied, the excitonic ground state is optically dark, and we conclude that it should remain so for all NC sizes. The explanation of the anomalous temperature dependence of radiative lifetimes in perovskite NCs must lie elsewhere and will be a subject of future investigation.

■ ASSOCIATED CONTENT

Data Availability Statement

An online repository of the codes and data used in this paper can be accessed at https://github.com/dgweinberg/perovNCs.

Supporting Information

The Supporting Information is available free of charge at https://pubs.acs.org/doi/10.1021/acs.nanolett.3c00861.

Additional details on the structural and electronic calculations, including the parametrization of pseudopotentials(PDF)

■ AUTHOR INFORMATION

Corresponding Authors

Daniel Weinberg − *Department of Chemistry, University of California, Berkeley, California 94720, United States; Materials Sciences Division, Lawrence Berkeley National Laboratory, Berkeley, California 94720, United States;* orcid.org/0000-0001-7552-4712; Email: d_weinberg@berkeley.edu

Eran Rabani − *Department of Chemistry, University of California, Berkeley, California 94720, United States; Materials Sciences Division, Lawrence Berkeley National Laboratory, Berkeley, California 94720, United States; The Raymond and Beverly Sackler Center of Computational Molecular and Materials Science, Tel Aviv University, Tel Aviv 69978, Israel;* orcid.org/0000-0003-2031-3525; Email: eran.rabani@berkeley.edu

Yoonjae Park − *Department of Chemistry, University of California, Berkeley, California 94720, United States; Materials Sciences Division, Lawrence Berkeley National Laboratory, Berkeley, California 94720, United States;* Email: yoonjae_park@berkeley.edu

David T. Limmer − *Department of Chemistry, University of California, Berkeley, California 94720, United States; Materials Sciences Division and Chemical Sciences Division, Lawrence Berkeley National Laboratory, Berkeley, California 94720, United States; Kavli Energy NanoScience Institute, Berkeley, California 94720, United States;* orcid.org/0000-0002-2766-0688; Email: dlimmer@berkeley.edu

Complete contact information is available at: https://pubs.acs.org/10.1021/acs.nanolett.3c00861

Notes

The authors declare no competing financial interest.

https://doi.org/10.1021/acs.nanolett.3c00861
Nano Lett. 2023, 23, 4997−5003

■ ACKNOWLEDGMENTS

This work was supported by the U.S. Department of Energy, Office of Science, Office of Basic Energy Sciences, Materials Sciences and Engineering Division, under Contract No. DE-461AC02-05-CH11231 within the Fundamentals of Semiconductor Nanowire Program (KCPY23).Methods used in this work were provided by the Center for Computational Study of Excited State Phenomena in Energy Materials (C2SEPEM), which is funded by the U.S. Department of Energy, Office of Science, Basic Energy Sciences, Materials Sciences and Engineering Division, via Contract No. DE-AC02-05CH11231 as part of the Computational Materials Sciences program. This research used resources of the National Energy Research Scientific Computing Center (NERSC), a U.S. Department of Energy Office of Science User Facility. D.W. is grateful for the mentorship and advice of John Philbin at the inception of this project and fruitful discussions with Ming Chen on the implementation of spin−orbit coupling. E.R. is grateful to Sasha Efros for fruitful discussions. We are thankful for useful conversations with Timothy Berkelbach.

■ REFERENCES

(1) Kovalenko, M. V.; Protesescu, L.; Bodnarchuk, M. I. Properties and potential optoelectronic applications of lead halide perovskite nanocrystals. *Science* **2017**, *358*, 745−750.
(2) Protesescu, L.; Yakunin, S.; Bodnarchuk, M. I.; Krieg, F.; Caputo, R.; Hendon, C. H.; Yang, R. X.; Walsh, A.; Kovalenko, M. V. Nanocrystals of Cesium Lead Halide Perovskites (CsPbX3, X = Cl, Br, and I): Novel Optoelectronic Materials Showing Bright Emission with Wide Color Gamut. *Nano Lett.* **2015**, *15*, 3692−3696.
(3) Schmidt, L. C.; Pertegás, A.; González-Carrero, S.; Malinkiewicz, O.; Agouram, S.; Mínguez Espallargas, G.; Bolink, H. J.; Galian, R. E.; Pérez-Prieto, J. Nontemplate Synthesis of CH3NH3PbBr3 Perovskite Nanoparticles. *J. Am. Chem. Soc.* **2014**, *136*, 850−853.
(4) Canneson, D.; Shornikova, E. V.; Yakovlev, D. R.; Rogge, T.; Mitioglu, A. A.; Ballottin, M. V.; Christianen, P. C. M.; Lhuillier, E.; Bayer, M.; Biadala, L. Negatively Charged and Dark Excitons in CsPbBr3 Perovskite Nanocrystals Revealed by High Magnetic Fields. *Nano Lett.* **2017**, *17*, 6177−6183.
(5) Becker, M. A.; et al. Bright triplet excitons in caesium lead halide perovskites. *Nature* **2018**, *553*, 189−193.
(6) Chen, L.; Li, B.; Zhang, C.; Huang, X.; Wang, X.; Xiao, M. Composition-Dependent Energy Splitting between Bright and Dark Excitons in Lead Halide Perovskite Nanocrystals. *Nano Lett.* **2018**, *18*, 2074−2080.
(7) Tamarat, P.; Bodnarchuk, M. I.; Trebbia, J.-B.; Erni, R.; Kovalenko, M. V.; Even, J.; Lounis, B. The ground exciton state of formamidinium lead bromide perovskite nanocrystals is a singlet dark state. *Nat. Mater.* **2019**, *18*, 717−724.
(8) Xu, K.; Vliem, J. F.; Meijerink, A. Long-Lived Dark Exciton Emission in Mn-Doped CsPbCl3 Perovskite Nanocrystals. *J. Phys. Chem. C* **2019**, *123*, 979−984.
(9) Rossi, D.; Liu, X.; Lee, Y.; Khurana, M.; Puthenpurayil, J.; Kim, K.; Akimov, A. V.; Cheon, J.; Son, D. H. Intense Dark Exciton Emission from Strongly Quantum-Confined CsPbBr3 Nanocrystals. *Nano Lett.* **2020**, *20*, 7321−7326.
(10) Rossi, D.; Qiao, T.; Liu, X.; Khurana, M.; Akimov, A. V.; Cheon, J.; Son, D. H. Size-dependent dark exciton properties in cesium lead halide perovskite quantum dots. *J. Chem. Phys.* **2020**, *153*, 184703.
(11) Nirmal, M.; Norris, D. J.; Kuno, M.; Bawendi, M. G.; Efros, A. L.; Rosen, M. Observation of the "Dark Exciton" in CdSe Quantum Dots. *Phys. Rev. Lett.* **1995**, *75*, 3728−3731.
(12) Sercel, P. C.; Lyons, J. L.; Wickramaratne, D.; Vaxenburg, R.; Bernstein, N.; Efros, A. L. Exciton Fine Structure in Perovskite Nanocrystals. *Nano Lett.* **2019**, *19*, 4068−4077.
(13) Aharonovich, I.; Englund, D.; Toth, M. Solid-state single-photon emitters. *Nat. Photonics* **2016**, *10*, 631−641.
(14) Park, Y.-S.; Guo, S.; Makarov, N. S.; Klimov, V. I. Room Temperature Single-Photon Emission from Individual Perovskite Quantum Dots. *ACS Nano* **2015**, *9*, 10386−10393.
(15) Utzat, H.; Sun, W.; Kaplan, A. E. K.; Krieg, F.; Ginterseder, M.; Spokoyny, B.; Klein, N. D.; Shulenberger, K. E.; Perkinson, C. F.; Kovalenko, M. V.; Bawendi, M. G. Coherent single-photon emission from colloidal lead halide perovskite quantum dots. *Science* **2019**, *363*, 1068−1072.
(16) Lv, Y.; Yin, C.; Zhang, C.; Yu, W. W.; Wang, X.; Zhang, Y.; Xiao, M. Quantum Interference in a Single Perovskite Nanocrystal. *Nano Lett.* **2019**, *19*, 4442−4447.
(17) Scholes, G. D.; Rumbles, G. Excitons in nanoscale systems. *Nat. Mater.* **2006**, *5*, 683−696.
(18) Park, Y.; Obliger, A.; Limmer, D. T. Nonlocal screening dictates the radiative lifetimes of excitations in lead halide perovskites. *Nano Lett.* **2022**, *22*, 2398−2404.
(19) Park, Y.; Limmer, D. T. Renormalization of excitonic properties by polar phonons. *J. Chem. Phys.* **2022**, *157*, 104116.
(20) Schilcher, M. J.; Robinson, P. J.; Abramovitch, D. J.; Tan, L. Z.; Rappe, A. M.; Reichman, D. R.; Egger, D. A. The significance of polarons and dynamic disorder in halide perovskites. *ACS Energy Letters* **2021**, *6*, 2162−2173.
(21) Mayers, M. Z.; Tan, L. Z.; Egger, D. A.; Rappe, A. M.; Reichman, D. R. How Lattice and Charge Fluctuations Control Carrier Dynamics in Halide Perovskites. *Nano Lett.* **2018**, *18*, 8041−8046.
(22) Brivio, F.; Butler, K. T.; Walsh, A.; van Schilfgaarde, M. Relativistic quasiparticle self-consistent electronic structure of hybrid halide perovskite photovoltaic absorbers. *Phys. Rev. B* **2014**, *89*, 155204.
(23) Dastidar, S.; Hawley, C. J.; Dillon, A. D.; Gutierrez-Perez, A. D.; Spanier, J. E.; Fafarman, A. T. Quantitative Phase-Change Thermodynamics and Metastability of Perovskite-Phase Cesium Lead Iodide. *J. Phys. Chem. Lett.* **2017**, *8*, 1278−1282.
(24) Quarti, C.; Mosconi, E.; Ball, J. M.; D'Innocenzo, V.; Tao, C.; Pathak, S.; Snaith, H. J.; Petrozza, A.; De Angelis, F. Structural and optical properties of methylammonium lead iodide across the tetragonal to cubic phase transition: implications for perovskite solar cells. *Energy Environ. Sci.* **2016**, *9*, 155−163.
(25) Han, Y.; Liang, W.; Lin, X.; Li, Y.; Sun, F.; Zhang, F.; Sercel, P. C.; Wu, K. Lattice distortion inducing exciton splitting and coherent quantum beating in CsPbI3 perovskite quantum dots. *Nat. Mater.* **2022**, *21*, 1282−1289.
(26) Tamarat, P.; Hou, L.; Trebbia, J.-B.; Swarnkar, A.; Biadala, L.; Louyer, Y.; Bodnarchuk, M. I.; Kovalenko, M. V.; Even, J.; Lounis, B. The dark exciton ground state promotes photon-pair emission in individual perovskite nanocrystals. *Nat. Commun.* **2020**, *11*, 6001.
(27) Rashba, E. I.; Sheka, V. Symmetry of Energy Bands in Crystals of Wurtzite Type II. Symmetry of Bands with Spin-Orbit Interaction Included. *Fiz. Tverd. Tela: Collected Papers* **1959**, *2*, 162−76.
(28) Hou, L.; Tamarat, P.; Lounis, B. Revealing the Exciton Fine Structure in Lead Halide Perovskite Nanocrystals. *Nanomaterials* **2021**, *11*, 1058.
(29) Sercel, P. C.; Lyons, J. L.; Bernstein, N.; Efros, A. L. Quasicubic model for metal halide perovskite nanocrystals. *J. Chem. Phys.* **2019**, *151*, 234106.
(30) Swift, M. W.; Lyons, J. L.; Efros, A. L.; Sercel, P. C. Rashba exciton in a 2D perovskite quantum dot. *Nanoscale* **2021**, *13*, 16769−16780.
(31) Quarti, C.; Giorgi, G.; Katan, C.; Even, J.; Palummo, M. Exciton Ground State Fine Structure and Excited States Landscape in Layered Halide Perovskites from Combined BSE Simulations and Symmetry Analysis. *Advanced Optical Materials* **2023**, 2202801.
(32) Biffi, G.; Cho, Y.; Krahne, R.; Berkelbach, T. C. Excitons and Their Fine Structure in Lead Halide Perovskite Nanocrystals from Atomistic GW/BSE Calculations. *J. Phys. Chem. C* **2023**, *127*, 1891−1898.

https://doi.org/10.1021/acs.nanolett.3c00861
Nano Lett. 2023, 23, 4997−5003

(33) Bischak, C. G.; Lai, M.; Fan, Z.; Lu, D.; David, P.; Dong, D.; Chen, H.; Etman, A. S.; Lei, T.; Sun, J.; Grünwald, M.; Limmer, D. T.; Yang, P.; Ginsberg, N. S. Liquid-like Interfaces Mediate Structural Phase Transitions in Lead Halide Perovskites. *Matter* **2020**, *3*, 534−545.
(34) Quan, L. N.; Park, Y.; Guo, P.; Gao, M.; Jin, J.; Huang, J.; Copper, J. K.; Schwartzberg, A.; Schaller, R.; Limmer, D. T.; et al. Vibrational relaxation dynamics in layered perovskite quantum wells. *Proc. Natl. Acad. Sci. U. S. A.* **2021**, *118*, No. e2104425118.
(35) Limmer, D. T.; Ginsberg, N. S. Photoinduced phase separation in the lead halides is a polaronic effect. *J. Chem. Phys.* **2020**, *152*, 230901.
(36) Swarnkar, A.; Marshall, A. R.; Sanehira, E. M.; Chernomordik, B. D.; Moore, D. T.; Christians, J. A.; Chakrabarti, T.; Luther, J. M. Quantum dot-induced phase stabilization of $CsPbI_3$ perovskite for high-efficiency photovoltaics. *Science* **2016**, *354*, 92−95.
(37) Zhao, Q.; Hazarika, A.; Schelhas, L. T.; Liu, J.; Gaulding, E. A.; Li, G.; Zhang, M.; Toney, M. F.; Sercel, P. C.; Luther, J. M. Size-Dependent Lattice Structure and Confinement Properties in CsPbI3 Perovskite Nanocrystals: Negative Surface Energy for Stabilization. *ACS Energy Letters* **2020**, *5*, 238−247.
(38) Yang, R. X.; Tan, L. Z. Understanding size dependence of phase stability and band gap in CsPbI3 perovskite nanocrystals. *J. Chem. Phys.* **2020**, *152*, 034702.
(39) Wang, L. W.; Zunger, A. Electronic Structure Pseudopotential Calculations of Large (∼ 1000 Atoms) Si Quantum Dots. *J. Phys. Chem.* **1994**, *98*, 2158−2165.
(40) Wang, L.-W.; Zunger, A. Pseudopotential calculations of nanoscale CdSe quantum dots. *Phys. Rev. B* **1996**, *53*, 9579−9582.
(41) Rabani, E.; Hetenyi, B.; Berne, B. J.; Brus, L. E. Electronic properties of CdSe nanocrystals in the absence and presence of a dielectric medium. *J. Chem. Phys.* **1999**, *110*, 5355−5369.
(42) Williamson, A.; Zunger, A. Pseudopotential study of electron-hole excitations in colloidal free-standing InAs quantum dots. *Phys. Rev. B* **2000**, *61*, 1978−1991.
(43) Rohlfing, M.; Louie, S. G. Electron-hole excitations and optical spectra from first principles. *Phys. Rev. B* **2000**, *62*, 4927−4944.
(44) Eshet, H.; Grünwald, M.; Rabani, E. The electronic structure of CdSe/CdS Core/shell seeded nanorods: Type-I or quasi-type-II? *Nano Lett.* **2013**, *13*, 5880−5885.
(45) Qiao, T.; Liu, X.; Rossi, D.; Khurana, M.; Lin, Y.; Wen, J.; Cheon, J.; Akimov, A. V.; Son, D. H. Magnetic Effect of Dopants on Bright and Dark Excitons in Strongly Confined Mn-Doped CsPbI3 Quantum Dots. *Nano Lett.* **2021**, *21*, 9543−9550.
(46) Shang, Q.; Kaledin, A. L.; Li, Q.; Lian, T. Size dependent charge separation and recombination in CsPbI3 perovskite quantum dots. *J. Chem. Phys.* **2019**, *151*, 074705.
(47) Yao, J.-S.; Ge, J.; Wang, K.-H.; Zhang, G.; Zhu, B.-S.; Chen, C.; Zhang, Q.; Luo, Y.; Yu, S.-H.; Yao, H.-B. Few-Nanometer-Sized α-CsPbI3 Quantum Dots Enabled by Strontium Substitution and Iodide Passivation for Efficient Red-Light Emitting Diodes. *J. Am. Chem. Soc.* **2019**, *141*, 2069−2079.
(48) Guvenc, C. M.; Yalcinkaya, Y.; Ozen, S.; Sahin, H.; Demir, M. M. Gd^{3+}-Doped α-CsPbI3 Nanocrystals with Better Phase Stability and Optical Properties. *J. Phys. Chem. C* **2019**, *123*, 24865−24872.
(49) Paul, S.; Samanta, A. Phase-Stable and Highly Luminescent CsPbI3 Perovskite Nanocrystals with Suppressed Photoluminescence Blinking. *J. Phys. Chem. Lett.* **2022**, *13*, 5742−5750.
(50) Franceschetti, A.; Zunger, A. Pseudopotential calculations of electron and hole addition spectra of InAs, InP, and Si quantum dots. *Phys. Rev. B* **2000**, *62*, 2614.
(51) Cho, Y.; Berkelbach, T. C. Environmentally sensitive theory of electronic and optical transitions in atomically thin semiconductors. *Phys. Rev. B* **2018**, *97*, 041409.
(52) Yin, C.; Chen, L.; Song, N.; Lv, Y.; Hu, F.; Sun, C.; Yu, W. W.; Zhang, C.; Wang, X.; Zhang, Y.; Xiao, M. Bright-Exciton Fine-Structure Splittings in Single Perovskite Nanocrystals. *Phys. Rev. Lett.* **2017**, *119*, 026401.
(53) Nestoklon, M. O.; Goupalov, S. V.; Dzhioev, R. I.; Ken, O. S.; Korenev, V. L.; Kusrayev, Y. G.; Sapega, V. F.; de Weerd, C.; Gomez, L.; Gregorkiewicz, T.; Lin, J.; Suenaga, K.; Fujiwara, Y.; Matyushkin, L. B.; Yassievich, I. N. Optical orientation and alignment of excitons in ensembles of inorganic perovskite nanocrystals. *Phys. Rev. B* **2018**, *97*, 235304.
(54) Yan, F.; Demir, H. V. LEDs using halide perovskite nanocrystal emitters. *Nanoscale* **2019**, *11*, 11402−11412.
(55) Kang, J.; Wang, L.-W. High Defect Tolerance in Lead Halide Perovskite CsPbBr3. *J. Phys. Chem. Lett.* **2017**, *8*, 489−493.
(56) Fu, M.; Tamarat, P.; Huang, H.; Even, J.; Rogach, A. L.; Lounis, B. Neutral and Charged Exciton Fine Structure in Single Lead Halide Perovskite Nanocrystals Revealed by Magneto-optical Spectroscopy. *Nano Lett.* **2017**, *17*, 2895−2901.
(57) Ramade, J.; Andriambariarijaona, L. M.; Steinmetz, V.; Goubet, N.; Legrand, L.; Barisien, T.; Bernardot, F.; Testelin, C.; Lhuillier, E.; Bramati, A.; Chamarro, M. Fine structure of excitons and electron−hole exchange energy in polymorphic CsPbBr3 single nanocrystals. *Nanoscale* **2018**, *10*, 6393−6401.

https://doi.org/10.1021/acs.nanolett.3c00861
Nano Lett. 2023, 23, 4997−5003